ELSEVIER

International Journal of Heat and Fluid Flow 22 (2001) 409–416

International Journal of HEAT AND FLUID FLOW

www.elsevier.com/locate/ijhff

On the flow structure within a turbulent spot

Mark W. Johnson *

Department of Engineering, The University of Liverpool, Liverpool L69 3GH, UK

Received 15 May 2000; accepted 23 December 2000

Abstract

A computational technique is presented for determining the fully three-dimensional viscid unsteady perturbation to a non-developing laminar boundary layer flow. The results reveal the strongly three-dimensional nature of the flow within a turbulent spot and its associated calmed region. Separation of the flow is found to occur along the demarcation line between the spot and the calmed region. This separation line advances downstream at the spot trailing edge velocity which is approximately half that of the freestream. In interpreting the results it was found convenient to consider the flow as seen by an observer travelling at the spot trailing edge velocity. From this viewpoint the unperturbed laminar boundary layer would consist of two fluid streams. A low momentum stream close to the wall which is travelling slower than the observer and hence approaches from downstream and a high momentum stream which is travelling more rapidly and hence approaches from upstream. The results show that once the flow is perturbed, the low momentum stream approaching the observer from downstream is deflected away from the surface close to the separation line and rolls up into a vortex at the rear of the spot. This vortex grows in both the streamwise and spanwise directions as more fluid is added from the low momentum stream. The high momentum stream drops towards the surface as it approaches the observer from upstream to fill the space vacated by the diverted low momentum stream. This results in the formation of the calmed region. The skin friction is increased within this region and hence some of the fluid from the high momentum stream is slowed to a velocity below that of the observer and hence moves back upstream. However, most of the high momentum stream continues towards the separation line where it is deflected away from the surface as it is entrained into the vortex. The vortex is therefore fed by both the low and the high momentum stream resulting in the high local transient shear rates typical of turbulent eddies. © 2001 Elsevier Science Inc. All rights reserved.

Keywords: Turbulence; Turbulent spot; Transition; Boundary layer; Turbulence generation; Turbulence modelling; Linear perturbation; Computational fluid dynamics

1. Introduction

The physical processes which lead to turbulence production are complex. For fluid dynamicists, turbulence was the 'chief outstanding difficulty of our subject' at the beginning of the last century (Lamb, 1916) and remained so at the end (Bradshaw, 1994). Despite the vast improvements in instrumentation, data analysis and computational methods, a complete understanding of the mechanisms of turbulence generation still eludes us. Direct numerical simulation (e.g. Rai and Moin, 1993) does now enable us to predict the effects of turbulence to high accuracy, but if methods of drag reduction (e.g. compliant surfaces, suction or riblets) are to be used to maximum effect a better understanding of the mechanisms of turbulence production and how drag reduction methods interact with them is vital.

Turbulent spots within transitional boundary layers were first identified by Emmons (1951). In the transition from a laminar boundary layer to a turbulent one, the initiation and growth of the spots plays a pivotal role. The first appearance of the turbulent spots determines the start of transition location and the subsequent growth in the spots dictates the length of the transition region prior to the fully turbulent boundary layer being achieved. The turbulent spot can therefore be considered as the key 'building block' of a turbulent boundary layer flow. A better understanding of the process of initiating a spot, whether through a Tollmien–Schlichting mechanism or through a Bypass mode, should therefore aid the prediction of start of transition. A better understanding of the flow mechanisms within the spot and how these lead to its development and growth would aid the prediction of transition length. Such knowledge is also valuable in understanding how turbulence is suppressed by, for example, streamwise acceleration during relaminarisation or by compliant surfaces.

Many researchers (e.g. Glezer et al., 1989; Gutmark and Blackwelder, 1987; Itsweire and Van Atta, 1984; Katz et al., 1990 and Sankaran et al., 1988) have used a variety of exper-

* Tel.: +44-151-794-4818; fax: +44-151-794-4848.
E-mail address: em22@liverpool.ac.uk (M.W. Johnson).

0142-727X/01/$ - see front matter © 2001 Elsevier Science Inc. All rights reserved.
PII: S0142-727X(01)00073-X

Notation

p'	fluctuating pressure
Re	boundary layer thickness Reynolds number ($= U\delta/\upsilon$)
Re_θ	momentum thickness boundary layer Reynolds number ($= U\theta/\upsilon$)
t	time
T	dimensionless time ($= Ut/\delta$)
u	time mean velocity in streamwise direction
U	freestream time mean velocity
u', v', w'	fluctuating velocities in x, y and z directions
v'_0	amplitude of initiating pulse at $X = 0, Y = 0, Z = 0$ and $T = 0$
x, y, z	streamwise, wall normal and spanwise coordinates
X, Y, Z	dimensionless coordinates ($= x/\delta, y/\delta$ and z/δ)
δ	boundary layer thickness
λ	Pohlhausen pressure gradient parameter
υ	kinematic viscosity
ρ	fluid density
Ω	vorticity

Subscripts

max	spatial maximum value
P	pulse width

imental techniques to study induced turbulent spots in laminar boundary layers. Ensemble averaging of a large number of spot realisations has revealed that the basic structure is that of a single horseshoe vortex tube (Itsweire and Van Atta, 1984). The spot itself has a planform similar to a triangular arrowhead, although a streamwise pressure gradient can lead to changes in this shape (Katz et al., 1990 and Gostelow et al., 1995). The trailing edge of the spot is almost invariant with both distance from the wall and spanwise position and has a convection velocity close to half the freestream velocity. The leading edge develops an overhang (Gutmark and Blackwelder, 1987) which travels at approximately 90% of the freestream velocity distant from the wall, but at a lower velocity close to the wall. Substructures, described as eddies, horseshoe or lambda vortices, have been identified within the spot (Sankaran et al., 1988) as being responsible for the generation of turbulence. The spot appears to grow through the addition of further substructures rather than the growth in the substructures themselves. These observations have helped to describe the structure of the turbulent spot, but as yet a clear understanding of the overall flow structure within the turbulent spot has not resulted.

The objective of the current work was to predict the flow within a turbulent spot in order that a clearer picture of the overall flow structure might be established and that the mechanisms leading to turbulence production could be better understood.

2. Equations of motion

In the current work, the unsteady flow is assumed to be a small linear perturbation to the time mean flow. For this reason only the primary instabilities within the flow are determined rather than full breakdown to turbulence. Nevertheless the characteristics of the linearly disturbed region are very similar to those of the turbulent spot as shown previously for Poiseuille flow by Li and Widnall (1989).

The time mean flow is considered to be inviscid and parallel and to have a Pohlhausen laminar profile:

$$\frac{u}{U} = 2\left(\frac{y}{\delta}\right) - 2\left(\frac{y}{\delta}\right)^3 + \left(\frac{y}{\delta}\right)^4 + \frac{\lambda}{6}\left(\left(\frac{y}{\delta}\right) - 3\left(\frac{y}{\delta}\right)^2 + 3\left(\frac{y}{\delta}\right)^3 - \left(\frac{y}{\delta}\right)^4\right). \tag{1}$$

The spot is assumed to be a small perturbation to this mean flow, but is considered to be fully three-dimensional and viscid. The unsteady momentum equations are

$$u'_t + \frac{1}{\rho}p'_x + uu'_x + u_y v' - \upsilon\nabla^2 u' = 0, \tag{2}$$

$$v'_t + \frac{1}{\rho}p'_y + uv'_x - \upsilon\nabla^2 v' = 0, \tag{3}$$

$$w'_t + \frac{1}{\rho}p'_z + uw'_x - \upsilon\nabla^2 w' = 0. \tag{4}$$

Applying continuity

$$u'_x + v'_y + w'_z = 0 \tag{5}$$

to the divergence of the momentum equations leads to

$$\frac{1}{\rho}\nabla^2 p' + 2u_y v'_x = 0. \tag{6}$$

Now differentiating this equation with respect to y and eliminating p' using the Laplacian of Eq. (3) yields

$$\nabla^2 v'_t + u\nabla^2 v'_x - u_{yy}v'_x - \upsilon\nabla^2(\nabla^2 v') = 0. \tag{7}$$

This equation is now written in terms of the dimensionless variables

$$X = \frac{x}{\delta}, \quad Y = \frac{y}{\delta}, \quad Z = \frac{z}{\delta} \quad \text{and} \quad T = \frac{Ut}{\delta} \tag{8}$$

as

$$\nabla^2 v'_T = -\frac{u}{U}\nabla^2 v'_X + \frac{u_{YY}}{U}v'_X + \frac{1}{Re}\nabla^2(\nabla^2 v'). \tag{9}$$

2.1. Boundary conditions

Boundary conditions are required on the wall and at the 'open' boundaries. On the wall, u', v' and w' will be zero and the y momentum equation reduces to

$$\frac{1}{\rho}p'_Y = \frac{1}{Re}v'_{YY} \tag{10}$$

whilst from the continuity equation $v'_Y = 0$.

Assuming the spot has not reached any of the open boundaries, it is reasonable to assume that u', v', w' and p' are zero and hence $v'_Y = 0$ on these boundaries.

2.2. Initial conditions

The turbulent spot is initiated by introducing a pulse at a point on the wall. This is analogous to the manner in which spots are induced in wind tunnel tests (e.g. Gostelow et al., 1995) where an electrical pulse excites a loudspeaker placed underneath a small hole in the wall on which a laminar

boundary layer is developing. In the current work, the pulse has a profile

$$\frac{v'}{v'_0} = \frac{1}{4}\left(1+\cos\frac{2\pi X}{X_P}\right)\left(1+\cos\frac{2\pi Z}{Z_P}\right) \tag{11}$$

for

$$\frac{-X_P}{2} \leqslant X \leqslant \frac{X_P}{2} \quad \text{and} \quad \frac{-Z_P}{2} \leqslant Z \leqslant \frac{Z_P}{2},$$

where X_P and Z_P are the pulse streamwise and spanwise widths. This may be shown to be equivalent to the Fourier expansion

$$\frac{v'}{v'_0} = \sum_{i=0}^{I}\sum_{k=0}^{K} \frac{1}{\pi^2(1-i^2(X_P/X_{\max})^2)(1-k^2(Z_P/Z_{\max})^2)} \times \sin\left(i\pi\left(\frac{X_P}{X_{\max}}\right)\right)\sin\left(k\pi\left(\frac{Z_P}{Z_{\max}}\right)\right)\cos\left(2\pi i\left(\frac{X}{X_{\max}}\right)\right) \times \cos\left(2\pi k\left(\frac{Z}{Z_{\max}}\right)\right). \tag{12}$$

3. Solution procedure

The coefficients of the unsteady flow field (u', v', w', p') in Eqs. (2)–(8) are functions only of Y, because of the assumption of a parallel steady flow field. For this reason it is convenient to use Fourier representations of u', v', w' and p' in the X and Z directions. Thus, making use also of the spanwise symmetry

$$q' = \sum_{i=0}^{I}\sum_{k=0}^{K}\left(q_c(i,k)\cos\frac{2\pi iX}{X_{\max}} + q_s(i,k)\sin\frac{2\pi iX}{X_{\max}}\right) \times \cos\frac{2\pi kZ}{Z_{\max}} \quad \text{for } q' = u', v' \text{ or } p'$$

and

$$q' = \sum_{i=0}^{I}\sum_{k=0}^{K}\left(q_c(i,k)\cos\frac{2\pi iX}{X_{\max}} + q_s(i,k)\sin\frac{2\pi iX}{X_{\max}}\right)\sin\frac{2\pi kZ}{Z_{\max}} \quad \text{for } q' = w', \tag{13}$$

where $q_c(i,k)$ and $q_s(i,k)$ are functions of Y alone.

Eq. (9) then becomes

$$(\nabla^2 v_c)_T = -\frac{u}{U}\frac{2\pi i}{X_{\max}}\nabla^2 v_s + \frac{u_{YY}}{U}\frac{2\pi i}{X_{\max}}v_s + \frac{1}{Re}\nabla^2(\nabla^2 v_c) \tag{14}$$

and

$$(\nabla^2 v_s)_T = \frac{u}{U}\frac{2\pi i}{X_{\max}}\nabla^2 v_c + \frac{u_{YY}}{U}\frac{2\pi i}{X_{\max}}v_c + \frac{1}{Re}\nabla^2(\nabla^2 v_s), \tag{15}$$

where

$$\nabla^2 = -\left[\left(\frac{2\pi i}{X_{\max}}\right)^2 + \left(\frac{2\pi k}{Z_{\max}}\right)^2\right] + \frac{\partial^2}{\partial y^2}.$$

Eqs. (2)–(4) can now also be written using dimensionless variables and Fourier representation, to yield

$$u_{cT} + \frac{2\pi iX}{X_{\max}}\left(\frac{1}{\rho}p_s + \frac{u}{U}u_s\right) + \frac{u_Y}{U}v_c - \frac{1}{Re}\nabla^2 u_c = 0, \tag{16}$$

$$u_{sT} - \frac{2\pi iX}{X_{\max}}\left(\frac{1}{\rho}p_c + \frac{u}{U}u_c\right) + \frac{u_Y}{U}v_s - \frac{1}{Re}\nabla^2 u_s = 0, \tag{17}$$

$$v_{cT} + \frac{1}{\rho}p_{cY} + \frac{u}{U}\frac{2\pi iX}{X_{\max}}v_s - \frac{1}{Re}\nabla^2 v_c = 0, \tag{18}$$

$$v_{sT} + \frac{1}{\rho}p_{sY} - \frac{u}{U}\frac{2\pi iX}{X_{\max}}v_c - \frac{1}{Re}\nabla^2 v_s = 0, \tag{19}$$

$$w_{cT} - \frac{1}{\rho}\frac{2\pi kZ}{Z_{\max}}p_c + \frac{u}{U}\frac{2\pi iX}{X_{\max}}w_s - \frac{1}{Re}\nabla^2 w_c = 0, \tag{20}$$

$$w_{sT} - \frac{1}{\rho}\frac{2\pi kZ}{Z_{\max}}p_s - \frac{u}{U}\frac{2\pi iX}{X_{\max}}w_c - \frac{1}{Re}\nabla^2 w_s = 0. \tag{21}$$

The Y and T derivatives in Eqs. (14)–(21) are now replaced by fourth and second-order finite difference expressions, respectively. At each time level and for each (i,k) Fourier term, Eqs. (14) and (15) are first solved to obtain values for v_c and v_s and then Eqs. (18) and (19) are solved to obtain p_c and p_s, Eqs. (16) and (17) for u_c and u_s and finally Eqs. (20) and (21) for w_c and w_s.

In the current work 31 grid points were used in the Y direction with 41 and 21 Fourier terms in the X and Z directions, respectively. The computational domain measured $40 \times 3 \times 20$ in the X, Y and Z directions. The computations were performed for a boundary layer Reynolds number $Re = 4000$, $Re_\theta = 470$ and with an initiating pulse measuring $X_P = 1$ and $Z_P = 1$ and $\Delta T = 0.1$ duration.

4. Results and discussion

4.1. Flow visualisation

The flow within the perturbed region is complex, strongly three-dimensional and time dependent. The author has found computer movies to be the most effective method of interpreting the results and the reader is encouraged to view a selection of these available on the author's web pages (Johnson, 2000). In this paper the figures are single frames taken from the streakline movies, which were produced by introducing a uniform matrix of particles at $T = 0$ and then plotting the position of each of these particles at subsequent times.

4.2. Geometry of the disturbed region

There are three characteristic velocities associated with the perturbed region. These are the velocities of the calmed region trailing edge, the spot trailing edge and the spot leading edge, which have typical values (Gostelow et al., 1995) of 20%, 50% and 90% of the freestream velocity. Clearly, the manner in which a particle will enter the perturbed region and move within it will depend on the range (0–20%, 20–50%, 50–90% or 90–100%) in which its initial (laminar) velocity lies. For this reason, particles originating from three levels within the boundary layer $Y = 0.1$, 0.3 and 0.7, which have initial velocities of 20%, 55% and 95% U, respectively, were used to study the perturbed flow. The streaklines are also drawn from the viewpoint of an observer who is moving at 50% of the freestream velocity, i.e. approximately with the calmed region/spot trailing edge interface.

The geometry of the spot and calmed region is apparent from the streaklines shown in the plan view of the perturbed region at $T = 40$ (Fig. 1). The boundary of the approximately circular calmed region is clearly marked out between $X = 8$ and 18 by the particles originating at $Y = 0.1$ and 0.3. These results show that low momentum fluid (originating from $Y = 0.1$) does not enter the calmed region, whereas the medium momentum fluid (from $Y = 0.3$) enters the region and is retained within it. The high momentum fluid (from $Y = 0.7$) passes through the calmed region with little apparent perturbation in its path.

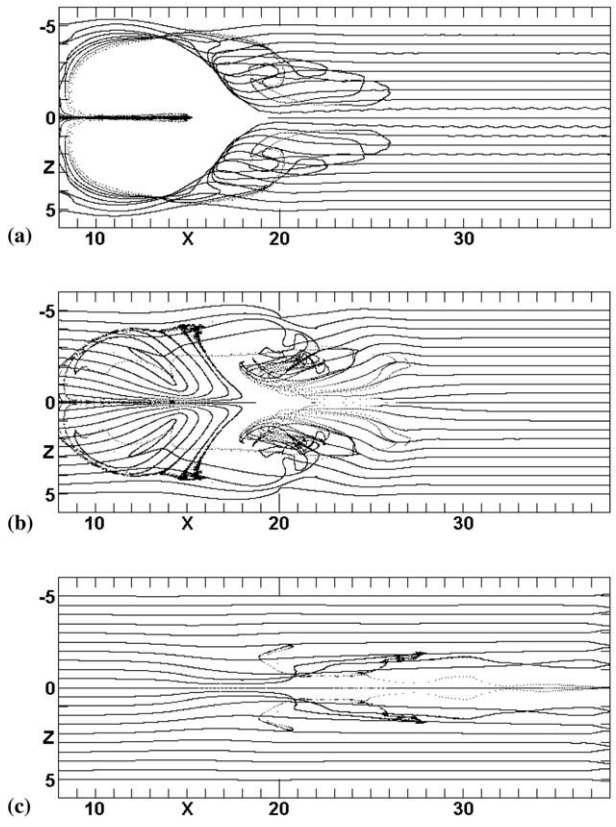

Fig. 1. Streaklines at $T = 40$. Particles originating from $Y = 0.1$ (a), $Y = 0.3$ (b) and $Y = 0.7$ (c).

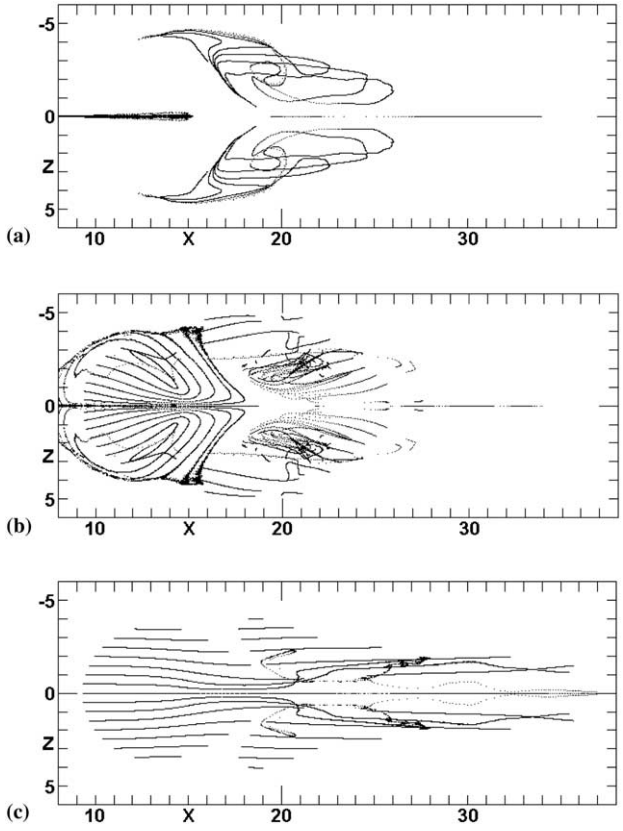

Fig. 2. Streaklines for particles that have changed height by more than $\Delta Y = 0.05$ at $T = 40$. Particles originating from $Y = 0.1$ (a), $Y = 0.3$ (b) and $Y = 0.7$ (c).

The edges of the spot are not clearly discernible in Fig. 1. The boundary is better defined in Fig. 2 where only particles which have changed their height above the plate by more or less than $\Delta Y = 0.05$ are shown. The characteristic triangular shape is depicted and the front overhang is also apparent as the spot extends further forward with increasing height from the plate. The streaklines within the spot are also more contorted than the more structured streaklines within the calmed region.

These results are therefore consistent with experimental results which depict similar geometries for the spot and calmed region plan views.

4.3. Basic flow structure

The plan view does not show the vertical movement of the particles which results in the momentum transfer or Reynolds stresses, which distinguish a turbulent flow from a laminar one. The vertical movement is shown in the side view of the streaklines on the symmetry ($Z = 0$) plane (Fig. 3). The lowest momentum fluid (originating from $Y < 0.1$) has a velocity less than the calmed region trailing edge and hence can only enter the perturbed region through the spot leading edge where it is then entrained upwards into the spot. As this low momentum fluid no longer enters the calmed region, higher momentum fluid (from $Y > 0.1$) descends towards the surface as it enters the calmed region from the rear to fill the resulting space. This leads to an increase in skin friction within the calmed region which decelerates the fluid closest to the wall such that it has insufficient velocity to reach the calmed region/spot interface. This fluid is therefore retained within the calmed region and increases its size. The highest momentum fluid (from $Y > 0.4$), on the other hand, has sufficient velocity to pass into the rear of the spot where it mixes with the low momentum stream entering the spot from upstream. The present results therefore support the view of Hofeldt et al. (1997), that the calmed region can be considered as a 'new' laminar boundary layer originating at the spot initiation site, in that although all the fluid forming the calmed region does not originate from the freestream, it does come from the freestream or upper part of the unperturbed boundary layer.

The reason for the very different characteristics of the calmed region and the spot is the sources of the fluid entering each. The calmed region only receives fluid from upstream. Although the fluid is perturbed, its laminar structure is maintained within the calmed region. In contrast the spot receives fluid from upstream and downstream. These two streams of fluid contain fluid of differing energies and hence when they are brought into close proximity within the spot high shear rates result which give rise to the eddies characteristic of a turbulent region.

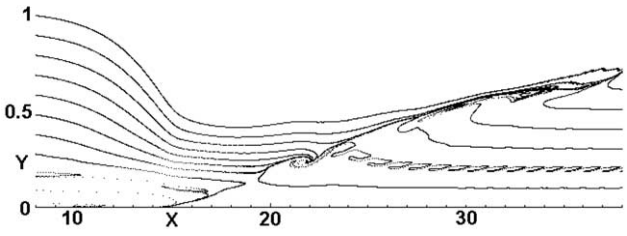

Fig. 3. Streaklines on symmetry ($Z = 0$) plane at $T = 40$.

4.4. Spot initiation

The formation of the spot requires that the low momentum fluid adjacent to the wall downstream of the spot is directed away from the wall as the spot passes over it. This can only occur if the low momentum fluid separates from the surface along the boundary between the spot and calmed region. A turbulent spot can therefore only be initiated when a local separation of the flow occurs as suggested by Smith et al. (1991) and Johnson (1994).

4.5. Three-dimensional structure

A two-dimensional (X–Z plane) flow structure has been outlined above. Although this is the underlying flow structure which governs the development of the spot and calmed region, the flow structure is also strongly three-dimensional.

Three-dimensional views of the streaklines originating at the three characteristic heights of $Y = 0.1$, 0.3 and 0.7 are shown in Fig. 4. The calmed region moves more rapidly than the fluid originating at $Y = 0.1$ and hence this region effectively moves through this fluid from left to right in Fig. 4. The leading edge of the calmed region deflects the slower moving fluid upwards where it rolls up in the spot to remain ahead of the advancing calmed region. It should be noted that the fluid passes underneath the spot almost unperturbed prior to be entrained into the roll up vortex close to the spot trailing edge. This is consistent with fluid which is within the viscous sublayer ($Y = 0.1$ is equivalent to $y^+ = 9$ at this Reynolds number).

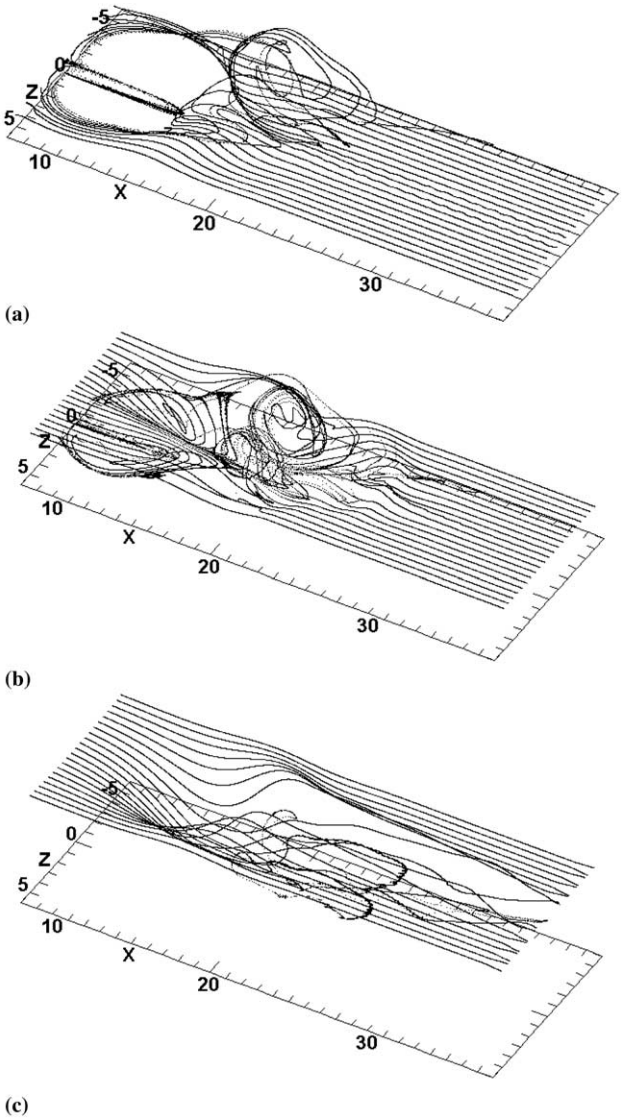

Fig. 4. Three-dimensional view of streaklines at $T = 40$. Particles originating from $Y = 0.1$ (a), $Y = 0.3$ (b) and $Y = 0.7$ (c).

Fluid originating from $Y = 0.3$ either enters the calmed region through its trailing edge or the spot through its leading edge dependent on whether the fluid was in front of or behind the perturbation at its initiation. The fluid entering the calmed region moves down towards the wall and also towards the centre line to replace the low momentum fluid entrained into the spot. As this fluid approaches the wall an increase in skin friction will result due to the increased shear and this decelerates the fluid such that it moves back and outwards towards the rear of the calmed region. This fluid thus forms a new fluid layer adjacent to the wall and expands the calmed region with time. The fluid originating from $Y = 0.7$ also dips towards the wall, but maintains sufficient velocity to pass through the calmed region to become entrained into the vortex at the rear of the spot. This vortex lifts this fluid away from the wall and at the same time moves it out from the centreline. The vortex is thus fed by low momentum fluid from downstream fluid which enters the front or bottom of the vortex and high momentum fluid which enters the top or rear of the vortex.

The leading edge of the spot is moving more rapidly than the laminar fluid at all Y levels less than about 0.9. The fluid initially ahead of the spot is therefore entrained into the spot as it is outrun. Fluid initially close to the wall passes beneath the spot before becoming entrained into the bottom of the vortex close to the spot trailing edge, whereas fluid further from the wall enters the spot closer to the spot leading edge.

4.6. The roll up or horseshoe vortex

The roll up or horseshoe vortex is responsible for the mixing of the low and high momentum streams entering the spot and hence is the source of the turbulence associated with the spot. The body of the vortex is located within the rear of the spot with the legs trailing back along the flanks of the calmed region to terminate on the surface. Low momentum fluid is entrained into the vortex from beneath whilst the higher momentum fluid enters from above. Once entrained the fluid spirals outwards from the vortex head towards its ends. The present results suggest that fluid entering the spot and entrained into the vortex will remain within the spot. The momentum transfer which occurs within the vortex increases the velocity of low momentum fluid above that of the spot trailing edge and decreases the velocity of high momentum fluid below that of the leading edge. No fluid is therefore permitted to travel back past the separation line into the calmed region or to travel forward through the spot leading edge.

4.7. Surface streak

The skin friction contours at $T = 40$ (Fig. 5) indicate that the highest levels of skin friction occur within a streak located along the centreline through the calmed region. This streak results when the high momentum stream converges in the spanwise direction as it impinges on the surface. These streaks are observed in surface visualisation experiments (e.g. Kittichaikarn et al., 1999).

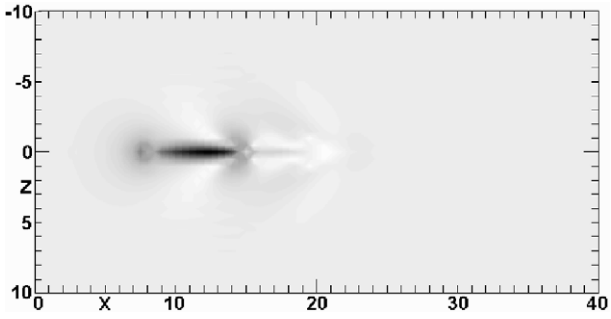

Fig. 5. Skin friction coefficient at $T = 40$. White is zero, black is $10 \times$ laminar value.

The current results suggest that most of the increase in skin friction within the perturbed region is due to the calmed region rather than the spot. Modest increases in skin friction occur beneath the spot as the low momentum stream passes beneath the spot as it accelerates due to mild convergence in the spanwise direction. There is also a significant region close to the spot calmed region interface where the skin friction is significantly reduced.

4.8. Effects of Reynolds number and pressure gradient

The effect of changing the boundary layer Reynolds number and the streamwise pressure gradient have been investigated. The effect of pressure gradient is strong with a substantial increase in the spot growth rate in adverse pressure gradients and a lesser decrease in favourable gradients (Johnson, 1998). An increase in Reynolds number increases the spot growth rate slightly (Johnson, 1999). In general the flow structure within the perturbed region is unaltered for favourable and mildly adverse pressure gradients, however the structure is altered when a strong adverse pressure gradient is experienced. Fig. 6 shows the plan view of the perturbed region for a $Re_\delta = 4000$ and $\lambda = -12$ ($Re_\theta = 456$) at $T = 40$. Again streaklines are chosen which have initial velocities close to the three characteristic velocities associated with the perturbed region and hence the streaklines originate from $Y = 0.2$, 0.4 and 0.7 where the velocity is 18%, 52% and 92% of the free-stream, respectively. When this figure is compared with the results for the zero pressure gradient case (Fig. 1), it is clear that the spot spreads more rapidly in the spanwise direction and also has a more rounded shape when an adverse pressure gradient is imposed as observed by Gostelow et al. (1995). The underlying flow structure within the spot is also altered though as shown by the streaklines on the symmetry plane ($Z = 0$) for the two cases (see Fig. 7). In the strong adverse pressure gradient the unperturbed flow contains much more low momentum fluid close to the wall; in order to accelerate this fluid above the spot trailing edge velocity, this must be mixed with a larger amount of high momentum fluid from the upper part of the boundary layer and the freestream within the spot. This process occurs in the horseshoe vortex located at the rear of the spot between $X = 15$ and 20. In the zero pressure gradient case (Fig. 3), the fluid entering the horseshoe vortex is rapidly convected down the vortex spiral away from the centreline. The vortex is unable to convect away the larger amount of fluid in the adverse pressure gradient case and hence the diameter of the vortex tube increases as more fluid is entrained and ultimately the horseshoe vortex becomes 'saturated'. A secondary calmed region/spot cell then forms ahead of the first. The calmed region does not develop however, as any high momentum fluid which decelerates as it approaches the wall is

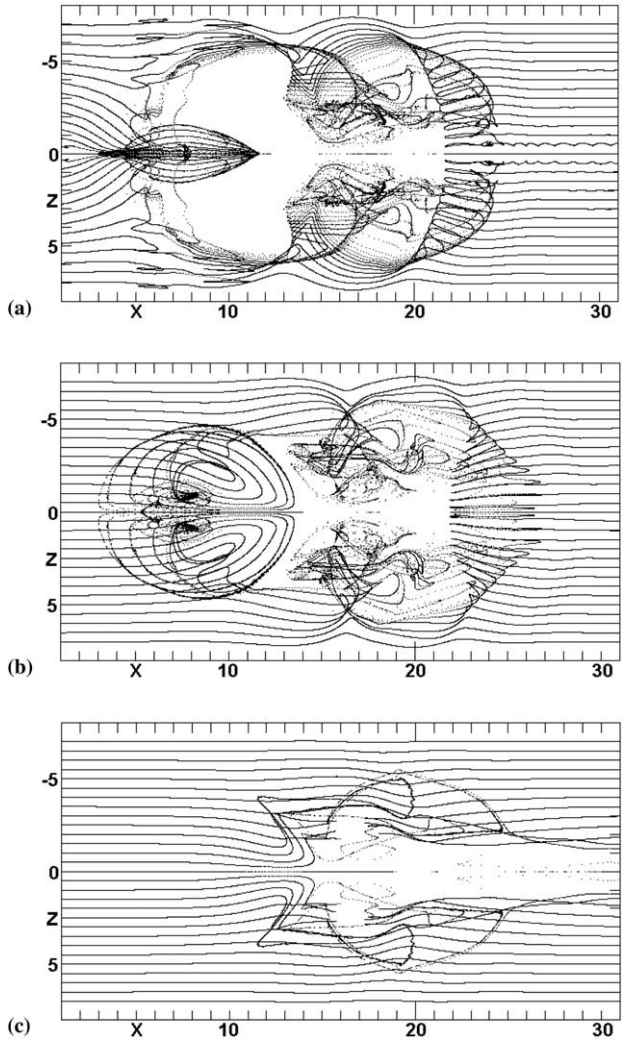

Fig. 6. Streaklines at $T = 40$ for $\lambda = -12$. Particles originating from $Y = 0.2$ (a), $Y = 0.4$ (b) and $Y = 0.7$ (c).

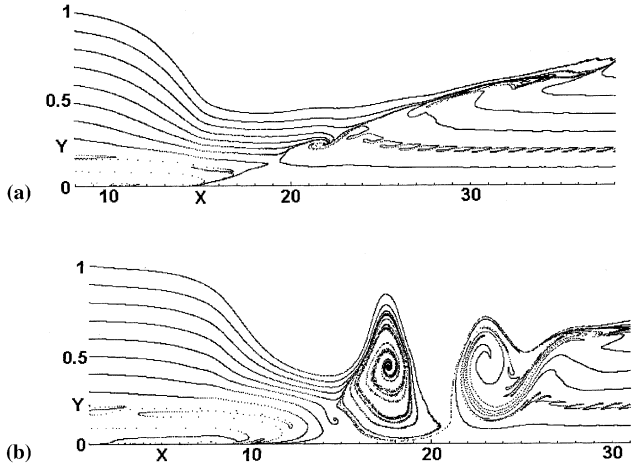

Fig. 7. Streaklines on symmetry ($Z = 0$) plane at $T = 40$. Zero pressure gradient (a) and string adverse pressure gradient (b).

entrained into the primary horseshoe vortex. The second vortex also develops and saturates in the same way leading to the formation of a third vortex. The spot therefore grows in the streamwise direction through the formation of additional horseshoe vortices rather than through the streamwise growth in a single vortex. The three-dimensional views in Fig. 8 show how the streaklines move outwards from the centreline along the horseshoe vortices more slowly than in the zero pressure gradient case. The calmed region retains its almost circular shape however.

4.9. Validity of a linear pertubation method

An exact analysis of the flow within a turbulent spot can only be achieved through a non-linear solution of the full Navier–Stokes equations, i.e. direct numerical simulation. It is therefore pertinent to consider the effect which the omission of the non-linear terms (i.e. $u'v'$ etc.) from Eqs. (2)–(4) has had on the accuracy of the current solutions. In two previous papers (Johnson, 1998, 1999), it has been shown that the predicted spot geometries agree with experimental findings within the experimental uncertainty. There is also, to the author's knowledge, no data from experimental or numerical studies which is inconsistent with the flow structure described in the current paper. The non-linear terms do, of course, contribute to the development of the perturbed region. They are responsible for introducing frequencies which are not present in the initiating perturbation and hence the current solutions. In particular the non-linear terms introduce the higher frequencies associated with turbulence. Nevertheless the magnitude of these non-linear terms is generally significantly smaller than the linear convection terms in Eqs. (2)–(4) and it is therefore reasonable to conclude that the overall flow structure within the spot is dominated and hence reasonably predicted by the linear terms alone.

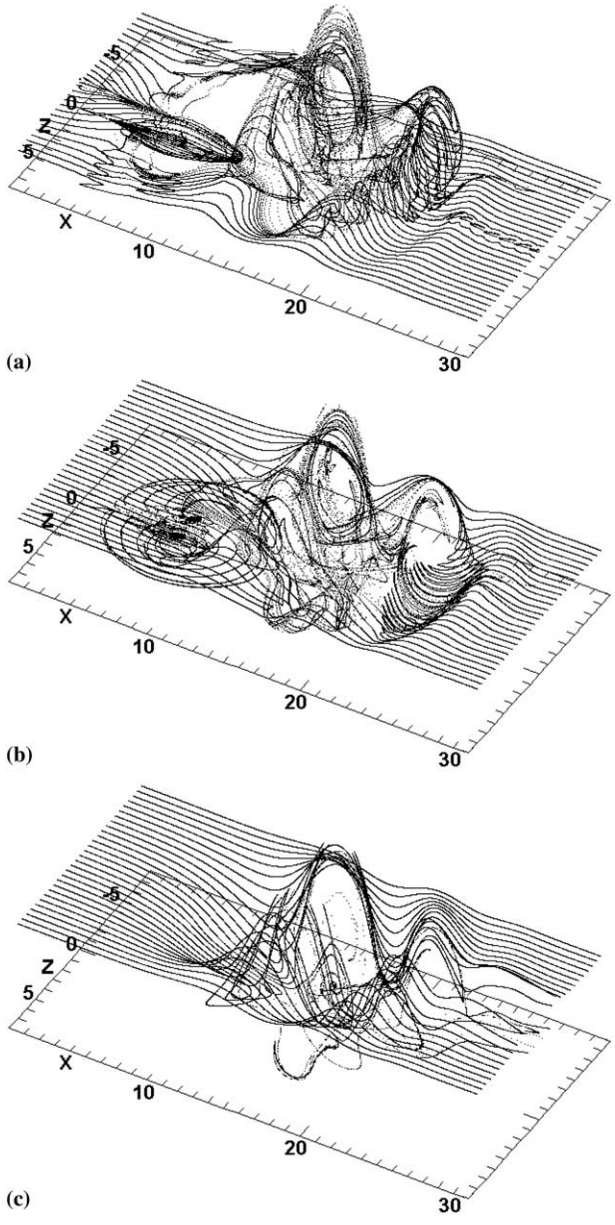

Fig. 8. Three-dimensional view of streaklines for adverse pressure gradient at $T = 40$. Particles originating from $Y = 0.2$ (a), $Y = 0.4$ (b) and $Y = 0.7$ (c).

5. Conclusion

(1) A method for predicting the fully three-dimensional viscid linear unsteady perturbation to a steady non-developing (inviscid) boundary layer is presented. The method is computationally simpler and much quicker than a full non-linear method and although the generation of turbulence cannot be predicted the geometric and structural development of the perturbation region strongly resembles a turbulent spot and its associated calmed region.

(2) Local separation of the flow is required to initiate a turbulent spot. Separation results in low momentum fluid being deflected away from the wall within the spot allowing higher momentum fluid to impinge upon the wall in the calmed region. Once this is effected, the low momentum fluid is accelerated through mixing and the high momentum fluid is decelerated through increased shear at the surface. This sustains the separation which grows in the spanwise direction as more fluid enters each region.

(3) The viscous sub-layer consists of fluid close to the wall which passes beneath the turbulent spot and is only entrained once it reaches the spot trailing edge. The horseshoe vortex, which generates the turbulence, does not extend down into the sub-layer.

(4) The turbulent spot is formed through the combination of a low and a high momentum stream of fluid. The low momentum stream passes into the spot through its leading edge and becomes entrained in the horseshoe vortex. The high momentum stream is drawn from the upper boundary layer and freestream and enters the rear of the spot. This fluid has passed through the calmed region before becoming entrained by the horseshoe vortex within the spot to combine with the low momentum stream. The turbulence observed within the spot occurs because of the high local shear stresses generated between these two streams of differing energy level.

(5) The calmed region results when high momentum fluid from the upper part of the laminar boundary layer descends towards the surface. The low momentum fluid present in the laminar layer does not enter the calmed region, but is diverted into the spot.

(6) The horseshoe vortex is located at the rear of the spot, with its legs trailing along the flanks of the calmed region to terminate at the wall. The horseshoe vortex is formed when fluid from a low momentum stream from downstream and a high momentum stream from upstream are rolled into the vortex. Once entrained, the fluid spirals outwards from the head of the vortex towards the legs. This vortex is the primary

source of turbulence generation which results from the high local shear rates induced due to the close proximity of the low and high momentum streams.

(7) In a strong adverse pressure gradient, the primary horseshoe vortex appears to become saturated by the larger amount of high momentum fluid which needs to be entrained in order to accelerate the larger amount of low momentum fluid present in the laminar adverse pressure gradient boundary layer. The spot grows in the streamwise direction through the development of additional horseshoe vortices which develop and saturate in a similar manner.

References

Bradshaw, P., 1994. Turbulence: the chief outstanding difficulty of our subject. Exp. Fluids 16, 203–216.

Emmons, H.W., 1951. The laminar-turbulent transition in a boundary layer – Part 1. J. Aero. Sci. 18, 490–498.

Glezer, A., Katz, Y., Wygnanski, I., 1989. On the breakdown of the wave packet trailing a turbulent spot in a laminar boundary layer. J. Fluid Mech. 198, 1–26.

Gostelow, J.P., Melwani, N., Walker, G.J., 1995. Effects of streamwise pressure gradient on turbulent spot development. ASME J. Turbomach. 118, 737–743.

Gutmark, E., Blackwelder, R.F., 1987. On the structure of a turbulent spot in a heated laminar boundary layer. Exp. Fluids 5, 217–229.

Hofeldt, A., Clark, J., LaGraff, J., Jones, T.V., 1997. The becalmed region in turbulent spots. In: Minnowbrook II: 1997 workshop on Boundary Layer Transition in Turbomachines, NASA/CP-1998-206958, pp. 95–98.

Itsweire, E.C., Van Atta, C.W., 1984. An experimental investigation of coherent substructures associated with turbulent spots in a laminar boundary layer. J. Fluid Mech. 148, 319–348.

Johnson, M.W., 1994. A bypass transition model for boundary layers. ASME J. Turbomach. 116, 759–764.

Johnson, M.W., 1998. Turbulent spot characteristics in boundary layers subjected to streamwise pressure gradient. ASME paper 98-GT–124.

Johnson, M.W., 1999. Prediction of turbulent spot growth rates. ASME paper 99-GT-031.

Johnson, M.W., 2000. Web page http://www.liv.ac.uk/~em22/home.html.

Katz, Y., Seifert, A., Wygnanski, I., 1990. On the evolution of a turbulent spot in a laminar boundary layer with a favourable pressure gradient. J. Fluid Mech. 221, 1–22.

Kittichaikarn, C., Ireland, P.T., Zhong, S., Hodson, H.P., 1999. An investigation on the onset of wake-induced transition and turbulent spot production rate using thermochromatic liquid crystals. ASME paper 99-GT-126.

Lamb, H., 1916. Hydrodynamics. Cambridge University Press, New York.

Li, F., Widnall, S.E., 1989. Wave patterns in plane Poiseuille flow created by concentrated disturbances. J. Fluid Mech. 208, 639–656.

Rai, M.M., Moin, P., 1993. Direct numerical simulation of transition and turbulance in a spatially evolving boundary layer. J. Compos. Phys. 109, 169–192.

Sankaran, R., Sokolov, M., Antonia, R.A., 1988. Substructures in a turbulent spot. J. Fluid Mech. 197, 389–414.

Smith, C.R., Walker, J.D.A., Haidari, A.H., Sobrun, U., 1991. On the dynamics of near wall turbulence. Philos. Trans. R. Soc. London A 336, 131–175.

Editorial postscript to "On the flow structure in a turbulent spot"

The preceding paper by Dr M.W. Johnson provoked highly contrasting reviews from referees of international standing. Briefly, two welcomed it as a significant breakthrough in providing a relatively simple approach to analysing the development of a turbulent spot while two others felt equally strongly that the approach was too simplistic to be of any general value. The Editors conferred and concluded that, in the interests of making the method known to the community, the paper should be published. We should however be interested to hear from readers who, having read the paper, wish to let us have their views either in support of the approach or opposed to it. It is hoped to include at least a representative selection of these responses in a future issue. Please send all communications, by mail, e-mail or fax, to Professor B.E. Launder.